Journal of Molecular Liquids 291 (2019) 111250

Contents lists available at ScienceDirect

Journal of Molecular Liquids

journal homepage: www.elsevier.com/locate/molliq

Bulk foam stability and rheological behavior of aqueous foams prepared by clay particles and alpha olefin sulfonate

Shuyan Chen [a], Hongjuan Liu [b], Jingjing Yang [a], Yujie Zhou [b,*], Jianan Zhang [b,*]

[a] Department of Environment and Quality Test, Chongqing Chemical Industry Vocational College, Chongqing 401228, China
[b] Institute of Nuclear and New Energy Technology, Tsinghua University, Beijing 100084, China

ARTICLE INFO

Article history:
Received 12 March 2019
Received in revised form 23 May 2019
Accepted 27 June 2019
Available online 28 June 2019

Keywords:
Enhanced oil recovery
Surfactant
Foam stability
Clay particle
Viscoelasticity

ABSTRACT

In recent years, nanoparticle-stabilized foam has become an important research domain to solve the foam stability issues under severe conditions because of its unique advantages. The aim of this study is to seek a better understanding for the application of foams stabilized by the mixtures of nanoparticles and anionic surfactant in chemical enhanced oil recovery (EOR). Properties of the aqueous foams prepared by alpha olefin sulfonate (AOS) and clay particle dispersions are examined using foam stability and rheological behavior analysis. The AOS/clay dispersions have a synergistic effect on the stability of foam and the foam stability increases with the clay particle concentration. Compared with surface charge, the hydrophobicity of particles directly influences foam stability and the most hydrophobic clay particles in AOS/clay dispersions own the most stable foams. With the addition of clay particles, the viscoelasticity modulus of both liquid film and bulk solution for AOS/clay dispersions are enhanced. The film damping coefficient results reveal that more energy from outside will be effectively used for AOS liquid film after the addition of clay particles. The clay particles are believed to stabilize foams by increasing extensional viscoelasticity modulus of AOS/clay dispersions and also by adsorbing on bubble surface, thus a three-dimensional network structure is formed between armored bubbles to slow bubble coalescence and disproportionation.

1. Introduction

As most of the oil field has entered the high water cut stage, chemical enhanced oil recovery (EOR) technologies are used to improve and stabilize the production of oilfields, which have become an important research topic in the modern petroleum industry [1–4]. More and more attention has been paid to variety of foam flooding recently in chemical EOR due to the unique seepage characteristics and oil displacement efficiency of foam flooding [5–7]. Foam can reduce the relative permeability of the gas-phase because of its high apparent viscosity, thus effectively controlling the mobility ratio in heterogeneous reservoirs. Meanwhile, foaming agents as the surfactants can lower the interfacial tension between oil and water [8–11], thus it can not only significantly improve the sweep efficiency, but also the microscopic oil displacement efficiency can be increased simultaneously. Therefore, foam flooding has a broad prospect of application in the chemical EOR.

Foam is essentially a thermodynamically unstable colloid system, and surfactants are the most commonly foaming agents for the preparation of foams currently. At present, one of the key issues for the successful application of foam flooding is foam stability [12–14]. The foam stability can be affected by a number of factors after being generated, such as the drainage of liquid, the gas diffusion between bubbles, the evaporation of water in the lamellae and the viscous forces, etc. [15]. Most of the research on foaming agents is focused on the synthesis of foaming agents or formula selection, the resulted foaming agents can produce enough foam volume, but the half-time of foam is short and the stability is poor [16,17]. Researchers have done numerous studies to improve the foam stability; the current common method is to use the polymers such as xanthan gum and partially hydrolyzed polyacrylamide to increase the viscosity of foaming agents, thus the stability of foam will be improved [18–21]. However, the polymers will be degraded along with the temperature, then the viscosity of polymers is decreased, resulting in a decrease in foam stability at high temperature. In addition, other chemicals can also be used along with surfactants to improve the foam stability [22–25]. When the water-soluble inorganic salts with suitable salinity are added into foaming agents, the electrical double layer will be compressed, resulting in a stable foam liquid membrane. However, the presence of inorganic salts can lead to the electrochemical corrosion of pipes and equipment.

Recently, the improvement of nanotechnology has made nanoparticles become a possibility to stabilize foam. Until now several studies on the use of particles and nanoparticles as stabilizers to produce

* Corresponding authors.
E-mail addresses: zhouyj@mail.tsinghua.edu.cn (Y. Zhou), zhangja@tsinghua.edu.cn (J. Zhang).

https://doi.org/10.1016/j.molliq.2019.111250
0167-7322/

ultrastable foams have been published, they are widely applied in food, cosmetics, minerals flotation, fire extinguishing and water-borne coatings [26–29]. Since Pickering and Ramsden discovered that proper wetting colloidal particles could stabilize emulsions by adsorbing on the gas-liquid interfaces to delay the drainage speed of liquid [30–32], the micro rod particles had been widely used as foam stabilizers in the conventional surfactants and surface-active polymers [33,34]. When suitable nanoparticles are added into the foam systems, they will be strongly adsorbed on the bubble surface, then a three-dimensional network is formed between the droplet surface and continuous phase to slow bubble coalescence and disproportionate, which is a key factor in the preparation of stable foams [35–37]. In most instances, only partially hydrophilic or hydrophobic particles can be adsorbed on the gas-liquid interfaces to stabilize foams, the contact angle between particles and gas-liquid interface determines the hydrophobicity of particles and it is very important for particles adsorbed on the gas-liquid interfaces [38–40]. Moreover, the particles can influence the rheological behavior of dispersive systems [41,42], thus affecting the viscoelastic properties of injected fluids, which also plays a crucial effect on improving the oil recovery efficiency in chemical EOR [43–45]. Zhang et al. [46] investigated foams stabilized by Laponite particles and cetyltrimethylammonium bromide (CTAB), and the results indicated that the particle/CTAB mixtures could greatly improve the foam stability at intermediate CTAB concentrations. Sharma et al. [47] found that the rheological properties of Pickering emulsion stabilized by the mixtures of clay-surfactant-polyacrylamide improved in contrast to conventional surfactant-polyether stable emulsions. Wang et al. [48] used experimental cores to investigate the blocking capacity and flow characteristics of nitrogen foam stabilized by the addition of clay particles. They found that the foam systems had the best blocking capacity in the cores at the foam quality of 0.74, and the foams could more effectively block channels in highly permeable cores compared to low permeability cores.

In this work, the stability and rheological behavior of foams generated by AOS surfactants and clay particles are examined in a series of experiments. First, the properties of AOS/clay dispersions were investigated. Second, the effects of zeta potential and hydrophobicity of clay particles on the stability (drainage half-life) of foams prepared by AOS/clay solutions were studied in detail. Finally, the rheological behavior of liquid film and bulk solution for AOS/clay dispersions were investigated systematically. And the stability mechanisms of foam prepared by AOS/clay dispersions were also discussed. The aim of this paper is seeking a better understanding for the application of particle-surfactant mixtures in chemical EOR.

2. Materials and methods

2.1. Materials

Alpha olefin sulfonate (AOS, $C_{14–16}$) with a molecular weight of 315 was received from Research Institute of Petroleum Exploration and Development (RIPED). The clay particles were also received from RIPED and they were made of rigid discoid montmorillonite crystals with the average diameter of 30 nm (Fig. 1). Distilled water was used in the following surfactant and/or clay solution systems. Both the surfactant and clay particles were used as received without further purification.

2.2. Methods

2.2.1. Preparation and characterization of AOS/clay aqueous dispersions

A certain amount of clay particles was dispersed into the distilled water for 2 h using a Multimixer (IKA, Germany), thus the clay dispersions were prepared. After that, the clay dispersions were sealed and laid aside at 25 °C for 3 days before used. Then, the AOS solution was added into the clay dispersion and the mixture continued with further stirring for 2 h to prepare the AOS/clay dispersions.

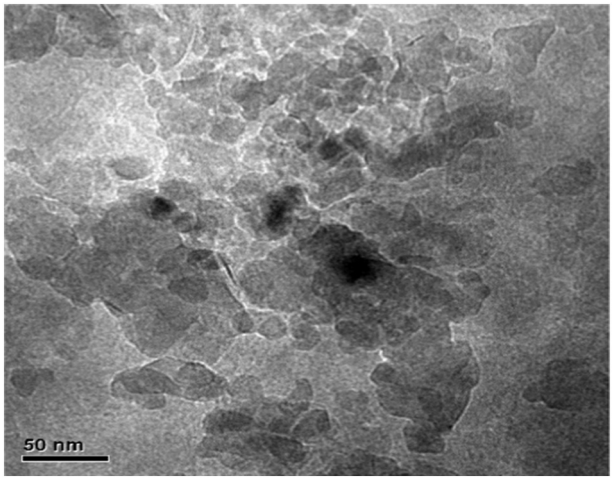

Fig. 1. Transmission Electron Microscopy (TEM) image of disk-shaped clay particles at the concentration of 0.1 wt% in distilled water.

The zeta potential of AOS/clay dispersions was measured using a Malvern Zetasizer Nano ZS90 instrument (USA). In the AOS/clay dispersions, the clay particle was fixed at 1.2 wt% while the AOS concentration was in the range of 0 wt% to 2.0 wt%. Each surfactant concentration was measured separately three times at least.

2.2.2. Air-water-clay contact angles

The three-phase contact angle of clay particles was determined though a Contact Angle measurement instrument (XG-CAMD, China) by the classic captive method. To reduce the errors caused by adsorption kinetics, the AOS/clay dispersions were first prepared and left for 24 h. Then, the AOS/clay dispersions were centrifuged and washed away the unattached AOS molecules with distilled water. After that, the clay particles in the sediment phase were dried at 80 °C and crushed into powers, and the powers were compressed into a circular disk with the thickness of about 1.0 mm. Then, a drop of water was dropped on the compressed disk surface, and the drip was photographed immediately. Thus, the three-phase contact angle of clay particles could be measured by a protractor.

2.2.3. Static bulk foam evaluation

The bulk foam stability experiments were measured by a stirring method using a Warring Blender (CPA6202S, USA), which were prepared by AOS solutions or AOS/clay dispersions, respectively. To create foam, 200 mL foaming agent solution was dumped into the container of Warring Blender, and the foam was generated for 60 s at 3000 rpm in this study. The foam volume decline was monitored over time after the foam generation. The initial foam volume (V_0) and the time for half volume dewatering (half-life, $t_{1/2}$) were used to investigate the foam stability. In this experiment, the concentration of clay particles varied from 0 to 0.5 wt% and the concentration of the surfactant AOS varied from 0 to 5 wt%. At the same time, a polarizing microscope (ZMP-203, Shanghai, China) was used to capture the photos of foam samples decaying after the foam generated.

2.2.4. Adsorption of particles on bubble surface

In this experiment, the laser-induced confocal microscope (TriM Scope, Germany) was used to investigate the adsorption of clay particle on bubble surfaces. The negatively charged Rhodamine B was used as the fluorescent probe and the maximum excitation wavelength was fixed at 543 nm. After the clay particles in the dispersion stained with Rhodamine B, the dispersions were centrifuged and washed by distilled water until the upper liquid was clarified. Foams stabilized with the dyed clay particles were prepared as described above and the fluorescent images of the foams could be obtained under the microscope.

2.2.5. Rheological characterization of bulk solution

The rheological behavior of clay or AOS/clay dispersions was carried out under room temperature being 20 ± 2 °C using the Haake rheometer (MARS, Thermo, Germany) equipped with a double concentric-cylinder (DG41). Both controlled rate (CR) and controlled stress (CS) test modes were used to record the flow curves. The steady shear viscosity experiments were implemented by the CR mode with the shear rate ranging from 0.01 s^{-1} to 200 s^{-1}. The small amplitude oscillatory shear experiment was performed by the Haake rheometer in order to decide the linear dynamic viscoelastic behavior. Also the linear viscoelastic region was decided by performing a strain sweep at 1.0 Hz for all samples. The storage moduli (G′) and the loss moduli (G″) were evaluated in a frequency range of 0.02 Hz to 10 Hz at the stress of 0.05 Pa. G′ and G″ represent the elastic and the viscous component of analyte, respectively. To make sure the same shear history, all test samples were laid aside 10 h after preparation and the samples were degassed by the vacuum for 0.5 h before rheological measurements.

2.2.6. The viscoelasticity modulus of liquid film tests

The homemade extensional viscoelasticity meter (FL10A, China) was used to investigate the dynamic tensile viscoelastic behavior of liquid films. And the tensile strain frequencies were set in the range of 0.2 Hz to 2.0 Hz. The results were analyzed according to the viscoelasticity modulus which contains the overall moduli (E), the storage moduli (E′), and the loss moduli (E″). Wherein, E′ and E″ represent the elastic and the viscous component of analyte, respectively. All the measurements were evaluated under room temperature of 20 °C for 150 s. The E, E′ and E″ are defined as follows:

$$E' = (\sigma_0/\varepsilon_0)\cos\delta \tag{1}$$

$$E'' = (\sigma_0/\varepsilon_0)\sin\delta \tag{2}$$

$$E = \sigma/\varepsilon = (\sigma_0/\varepsilon_0) \times \exp(i\delta) = (\sigma_0/\varepsilon_0) \times (\cos\delta + i\sin\delta) = E' + iE'' \tag{3}$$

Wherein, σ_0 is the maximum of stress; ε_0 is the maximum of strain; δ is phase-shift angle of the responses of stress and strain.

In the study of polymer viscoelasticity, tanθ is usually referred to as internal friction. For liquid film in this article, the ratio of loss modulus to storage modulus tanθ is similarly defined as film damping coefficient. It reflects the relationship between energy lost and stored in the liquid film. The energy distribution of the liquid film in a sinusoidal exciting cycle can be characterized by the value of tanθ. The value of tanθ equals to 1.0 (E″ = E′) can be considered as a watershed of energy distribution for liquid film. When the tanθ is <1.0 (E″ < E′), it indicates that the energy lost portion is less than energy stored in one sinusoidal cycle. On the contrary, when the tanθ is higher than 1.0 (E″ > E′), it indicates that the energy lost is larger than energy stored in one sinusoidal cycle. The tanθ is defined as follows:

$$\tan\theta = E''/E' \tag{4}$$

3. Results and discussion

3.1. Zeta potentials of AOS/clay aqueous dispersions

The zeta potentials can reflect the adsorption of particles on the stern plane and can be used as an indicator for the stability of colloid systems. The electrophoretic measurements were tested with clay particle dispersions as a function of AOS concentration, and the results were shown in Fig. 2. It could be seen that the zeta potential of clay particles was −43 mV in the absence of AOS. At lower AOS concentrations, the zeta potential value of particles increased obviously with AOS concentration. Although the zeta potential indicates that the net charge of clay particle is negative charge, it has been reported that the clay has heterogeneous distribution of surface charges, there still exists significant amount of cationic binding sites in the clay surfaces, which can interact with anionic surfactants [49–51]. In this case, the anionic surfactant AOS molecules can be adsorbed onto the clay particles because of the clay containing positively charged sites, and the adsorption amount of the AOS molecules on clay particles gradually increased with the AOS concentration. Therefore, the zeta potential of the particles increased gradually after the adsorption of AOS molecules. When the AOS concentration was 1.0 wt%, the zeta potential of clay particles reached the maximum value. After that, the zeta potential of clay particles tended to be constant and finally decreased slightly. It is because that the AOS molecules form a dense adsorption layer on the clay particles surface after the AOS concentration exceeded 1.0 wt%, and the zeta potential value of clay particles will no longer change greatly when the adsorption amount of AOS molecules on the clay particles reaches saturation.

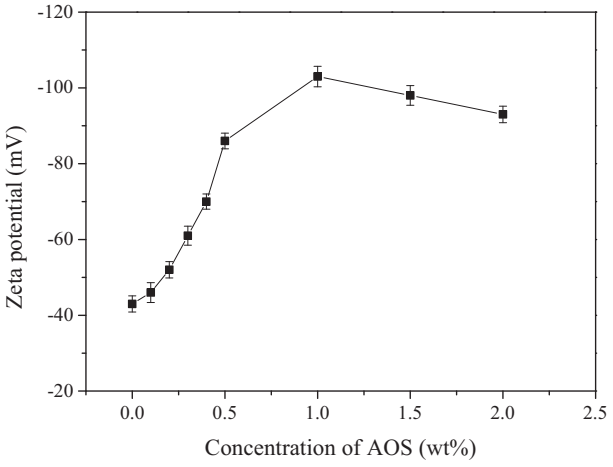

Fig. 2. Zeta potential of AOS/clay aqueous dispersions.

3.2. Hydrophobicity of modified particles

Since the contact angle can directly describe the hydrophily or hydrophobicity of particles, so it is a crucial indicator in judging particles adsorbed on the gas-liquid interface and the foam stability [52,53]. Fig. 3 showed the effects of AOS concentration on the wettability of clay particles. It could be found that the initial contact angle of clay particles was <20° in the free of AOS, which indicates that the clay particles

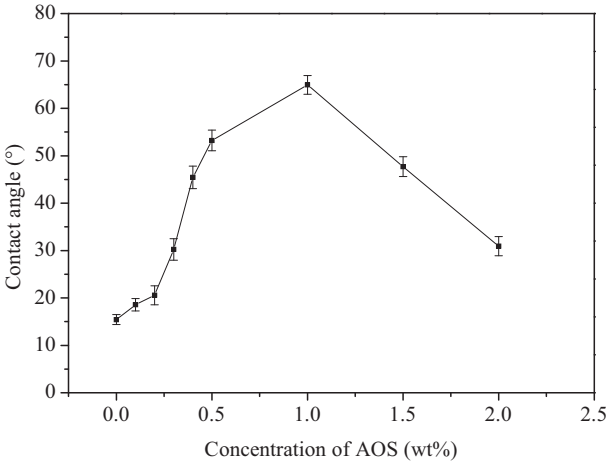

Fig. 3. Three-phase contact angle of particles as a function of AOS concentration.

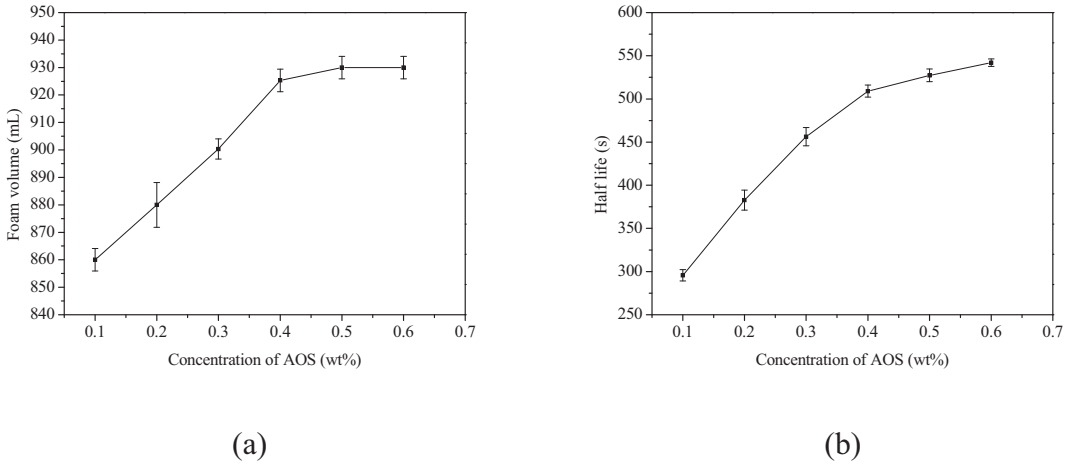

Fig. 4. The initial foam volume (a) and half-life (b) of AOS foam.

are hydrophilic. After the addition of AOS, the adsorption amount of AOS molecules on the gas-liquid interface of clay particles increases with the AOS concentration, resulting in an increase in the contact angle and there was a maximum value of 65° at 1.0 wt% of AOS. Then, the contact angle decreased with the increase of AOS concentration. Thus, the clay particles undergo a transition from hydrophilic to more hydrophobic to hydrophilic again. Solid particles can effectively wrap the droplets of dispersed phase in the liquid/liquid interface through space/electrostatic interaction, so as to stabilize the dispersed phase. The stability of droplets in dispersed phase is depended on the wetting balance of solid particles in two phases. When the contact angle of solid particles approaches 90°, the forming emulsion system has the best adhesive property and the formed emulsion is most stable. If the solid particles are completely wetted by aqueous phase or oil phase, the solid particles will be completely dispersed in aqueous phase or oil phase and will not form stable emulsion systems [54]. It can be seen that the contact angle of clay particles modified by AOS surfactant gradually increases so that the contact surface of clay particles will undergo wettability alteration.

3.3. Properties of foams stabilized by AOS and clay particles

3.3.1. Static stability of bulk foams

In order to get direct information about the effects of AOS surfactants and clay particles on foam stability, the foams stabilized by AOS solution or clay particles alone were investigated firstly. Clay particles are very hydrophilic and they are poor foaming agent. The aqueous dispersions prepared by clay particles with a concentration of 0.5 wt% solely did not result in any foam formation. The foamability and stability of foams prepared by AOS solution were shown in Fig. 4. It could be seen that the AOS solution rapidly formed foam and the foam volume first increased with the AOS concentration, then remained almost the same when the AOS concentration exceeded 0.4 wt% (Fig. 4(a)). Similar results were also found with the stability of AOS foams (Fig. 4(b)). It is observed that the foam volume reduces with elapse of time continuously, and the lower AOS concentration has no effect on extending the half-life of foam. The AOS-stabilized foam was unstable, the bubble coalescence and breakage resulted in quick loss of the foam volume even if the AOS concentration exceeded 0.4 wt%, the foam was fully collapsed after 4 h.

However, in most cases only surfactant is difficult to obtain the satisfactory stable foam, such as the heavy oil reservoirs with high temperature and high pressure. In such condition, the addition of nanoparticles from outside into foam formula can enhance the stability of foams. The foamability and stability of foams prepared from the mixtures of AOS solution (0.4 wt%) and increasing concentrations of clay particles were shown in Fig. 5. The concentration of clay particles in the dispersions varied from 0 to 1.6 wt%. As demonstrated in Fig. 5(b), the half-life of foams increased significantly after the introduction of clay particles in contrast to the AOS-stabilized foam. Particularly, the half-life of foam increased from 525 s to 3405 s after the addition of 1.6 wt% clay particles, which indicates that the AOS/clay dispersions have a synergistic effect on the foam stability. And the foams stabilized by AOS/clay mixtures can maintain the initial foam height for months if the glass is sealed to avoid evaporation. However, the presence of clay particles also influenced foamability of AOS (Fig. 5(a)). The foam volume decreased

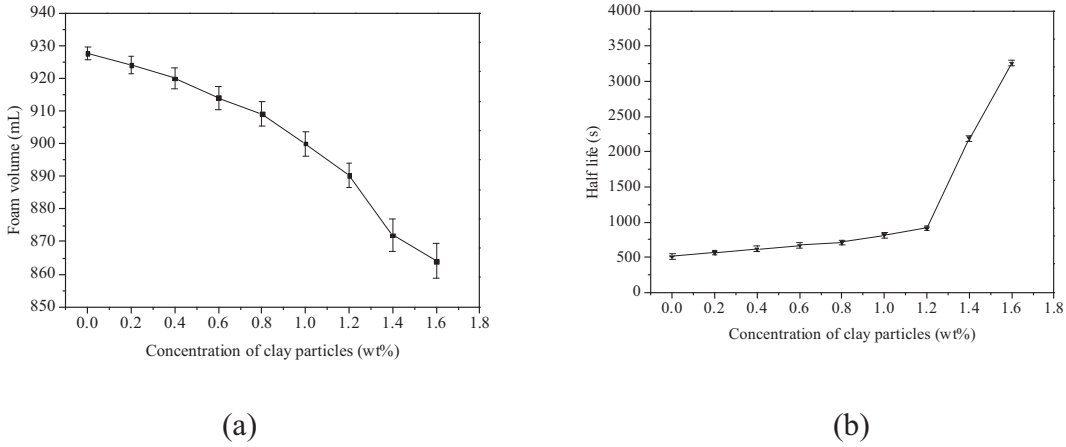

Fig. 5. The initial foam volume (a) and half-life (b) of foams stabilized by the mixtures of AOS solution (0.4 wt%) and clay particles as a function of clay particle concentration.

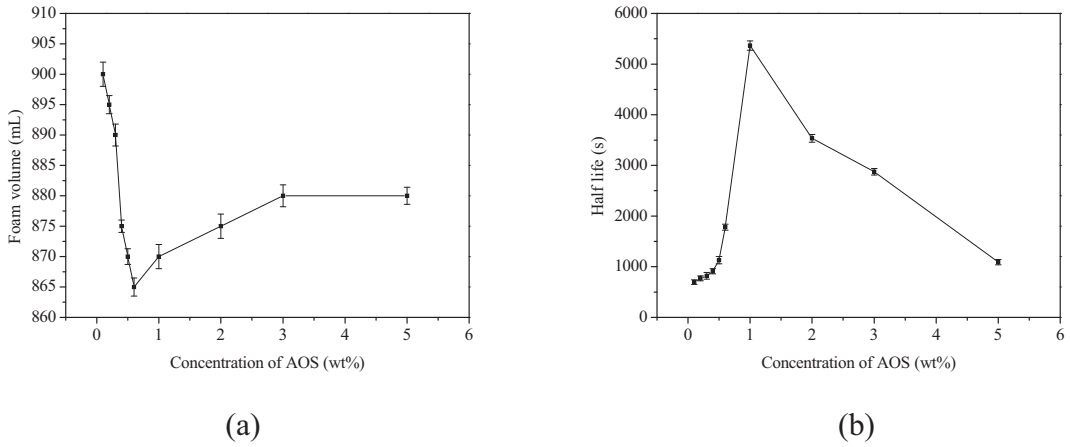

Fig. 6. The initial foam volume (a) and half-life (b) of foams stabilized with AOS/clay dispersion as a function of AOS concentration.

obviously from 925 mL to 865 mL after the addition of 1.6 wt% clay particles, which indicates that the adverse effects of clay particles should be considered carefully.

To deeply understand how the AOS/clay mixtures influence the foam stability, detailed information about the foams from the mixtures of clay particles (1.2 wt%) and an increased concentration of AOS prepared and the obtained results were shown in Fig. 6. The concentration of AOS in the dispersions varied from 0.1 wt% to 5.0 wt%. From Fig. 6 (a) it could be seen that the initial foam volume decreased firstly and then increased with the AOS concentration, and the foam volume was the smallest when the AOS concentration was 0.6 wt%. As an overall trend, although the addition of clay particles results in a lower foam volume, the effect of AOS concentration on foam volume is very small in the experimental AOS concentration range. In AOS/clay dispersions, the stability of foams increased continuously with the AOS concentration and reached a maximum value of 5370 s at 1.0 wt% of AOS, then decreased gradually when the AOS concentration exceeded this (Fig. 6 (b)). It is very different from the foam stability discussed previously for AOS-only foams and the AOS/clay dispersions (AOS concentration was fixed). When the AOS concentration was higher than 1.0 wt%, it was distinct that the introduction of clay particles obviously decreased the stability of AOS foam.

The adsorption of AOS molecules on clay particles may be responsible for the foam stability. At low AOS concentrations (0.1 wt% to 0.4 wt %), AOS molecules are adsorbed on the clay particles because of the electrical property and Van der Walls force between the surfactant

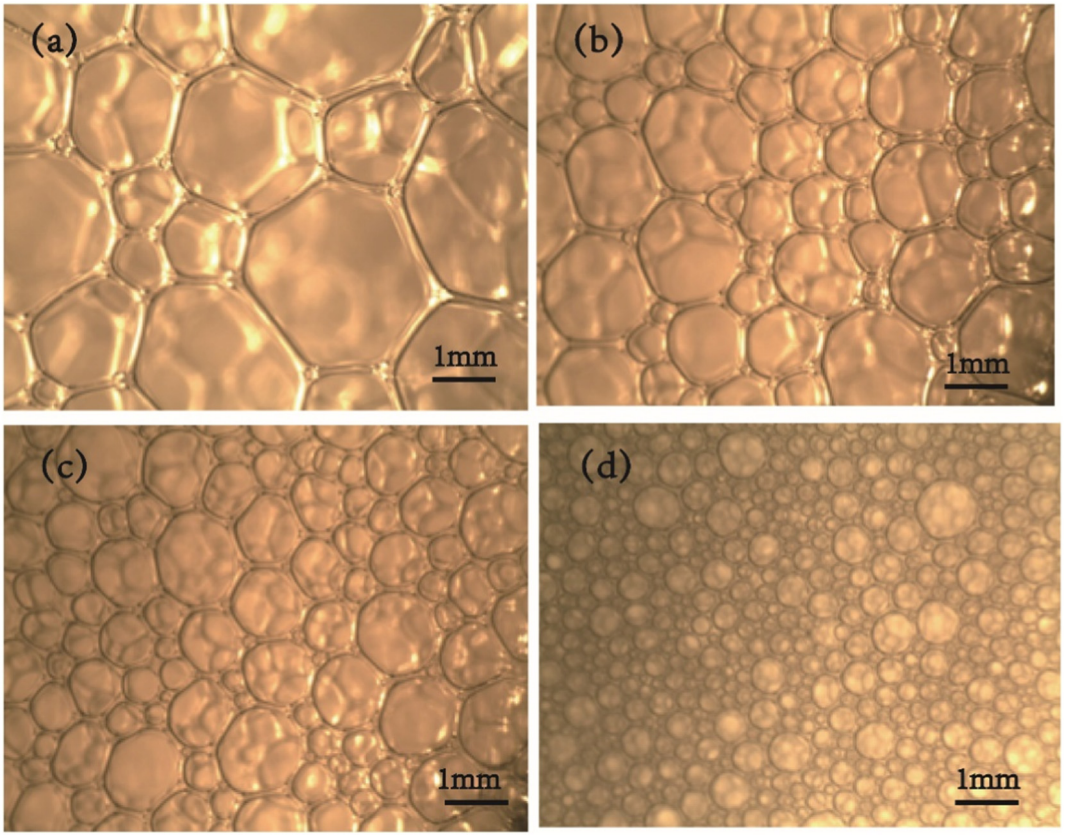

Fig. 7. Optical microscopy images of bubbles stabilized by 0.4 wt% of AOS alone (a) (10 min after formation) and by AOS/clay mixtures at clay concentrations of (b) 0.4 wt%, (c) 0.8 wt% and (d) 1.2 wt% (30 min after formation).

molecular and particle surface. The dispersions are stable and the stability of foams is similar to that of AOS-stabilized foam. At intermediate AOS concentrations (0.5 wt% to 1.5 wt%), the clay particles coating with a surfactant monolayer are aggregated along with the increase of hydrophobicity. So, the adsorption of AOS molecules on clay particles is driven by the repulsive interactions between particles and the head groups of AOS molecules, rather than electrostatic interaction. And the patches of two-dimensional aggregates on the clay surfaces are formed. As the AOS molecules continue to adsorb on the surface of clay particles, the micelles appear and lead to an increase in the negative charge density of the clay surface, further increasing the repulsive interaction between clay particles, therefore the stability of foam system was enhanced. Foams were most stable at 1.0 wt% of AOS, which corresponded to the concentration at which the hydrophobicity of clay particles reached the maximum value (Fig. 3). When AOS concentration exceeded 1.0 wt%, the zeta potential of clay particles changes little (Fig. 2), while the hydrophobicity of clay particle reduces with AOS concentration. It indicates that the electrostatic repulsion between the particles is almost constant and the hydrophobic attraction interaction between the particles is reduced. At this time, the change of the zeta potential is small, and the hydrophobic attraction interaction between the particles is dominant here, which can impair the foam stability. This can also be seen from the variation of foam stability of AOS/clay dispersions as a function of AOS concentration shown in Fig. 6. From the above analysis, it can be concluded that in terms of the stability of the particle-stabilized foam systems, the hydrophobicity of particles is more important than the surface charge of particles. The increase in hydrophobicity of the particles and the hydrophobic attraction interaction between the particles increase the density of the particles adsorbed on the surface of the bubbles, thereby increasing the stability of the foams. The stability of foams prepared by the mixtures of AOS and clay particles increases with increasing the hydrophobicity of particles. At high AOS concentrations (>1.5 wt%), a second layer of surfactant molecules with head groups oriented toward the aqueous solution forms on the clay particle surfaces, which decreases the hydrophobicity of particles and reduces the tendency of particles adsorbed on the bubble surfaces. Therefore, the foam stability declines especially as the clay particles are replaced by monomeric surfactant and cannot be adsorbed on the air-water interfaces, resulting of the foams are stabilized by AOS molecules only. It can be concluded that foam stability is related to the adsorption of AOS molecules on clay particles.

3.3.2. Adsorption of particles on the bubble surface

The hydrophobicity of clay particles is changed by the adsorption of AOS molecules on clay surfaces, as a result, partial hydrophobic clay particles is able to adsorb on the air bubbles. To investigate the adsorption of particles on gas-liquid surface, the optical microscope experiments were performed firstly and the microscopic images from generated foams by AOS/clay dispersions were demonstrated in Fig. 7. As observed, the shapes and sizes of bubbles in foams stabilized by AOS/clay dispersions both were different from that of foams stabilized by AOS alone. And the morphology of bubbles became smaller after the addition of clay particles. The bubble size of foam decreased gradually with increasing the clay concentration. The smallest of bubble size, the most stable of foam. This result is accordant to the stability of bulk foam.

In order to probe the adsorption of particles on bubble surface, the laser-induced confocal scanning microscopy experiments were performed and the results were shown in Fig. 8. It could be seen that the

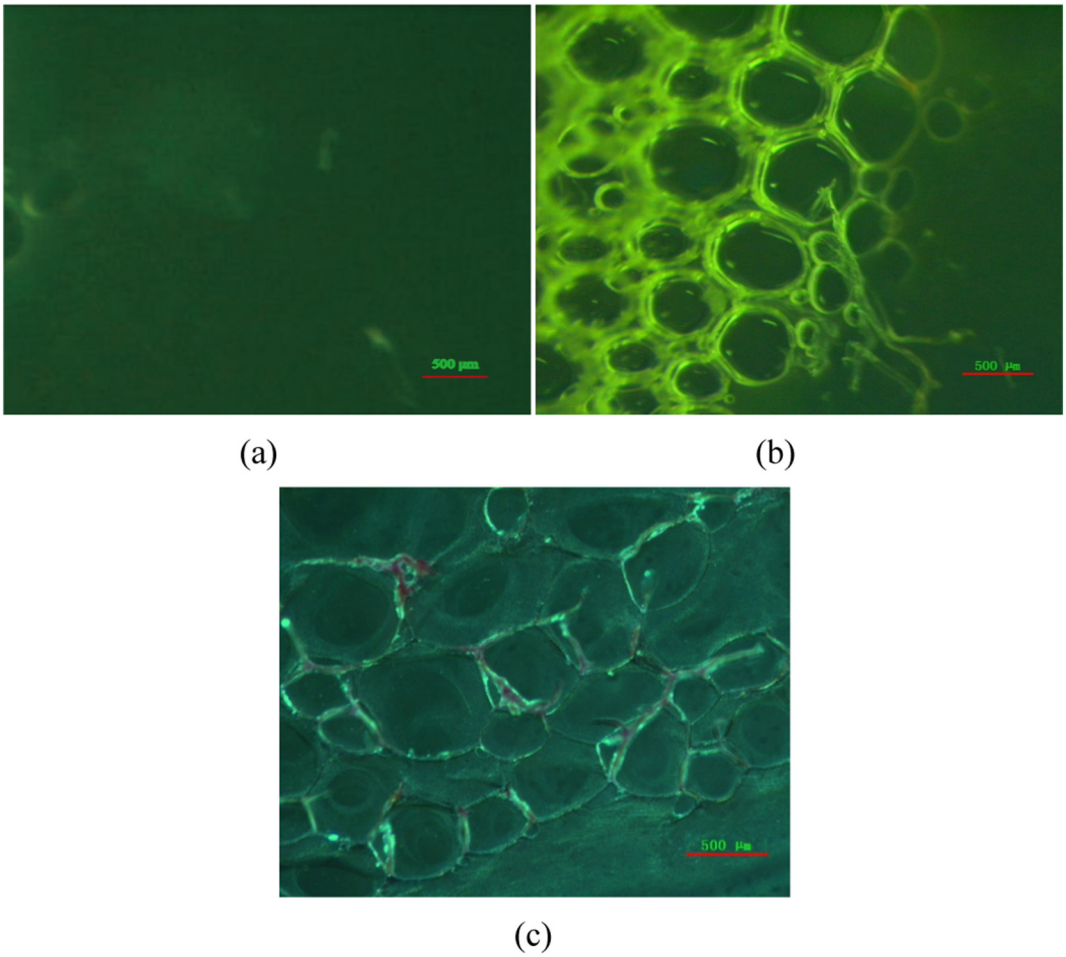

Fig. 8. Confocal fluorescence image for the foams stabilized by AOS only (a) and fluorescently labeled AOS-modified clay particles (b and c). (b): wet foams; (c): dry foams.

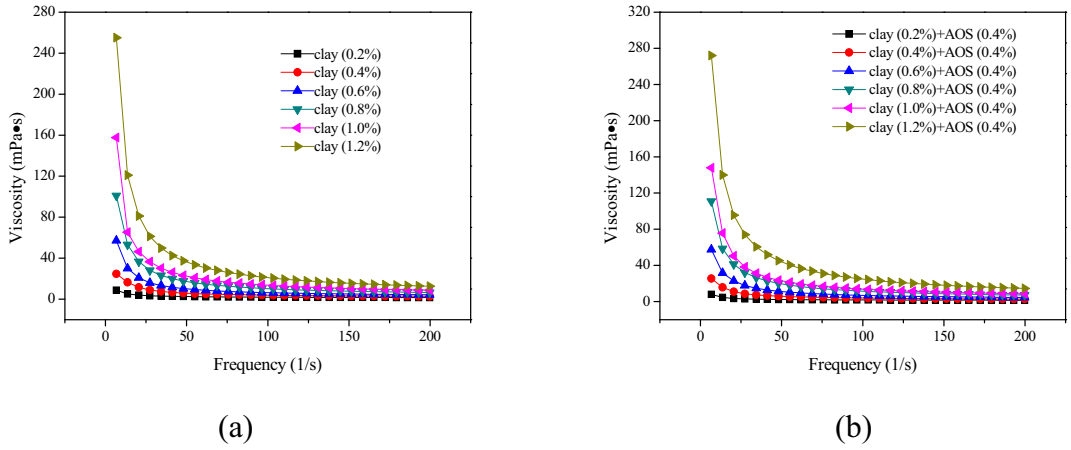

Fig. 9. The effect of frequency on the apparent viscosity of varies concentrations of clay dispersion (a) and AOS/clay dispersion (b).

structure of the foam stabilized by the fluorescently labeled AOS-modified clay particles (Fig. 8(b)) is clearly visible using the fluorescence confocal microscope in contrast to that of foam stabilized by AOS only (Fig. 8(a)). The clay particles are adsorbed on the bubble surfaces, and partial particles exist in the lamellas which are separated by the Plateau borders. Therefore, the clay particles of bulk solution can urge the bubbles connect up to form a three-dimensional network structure, thus the foam stability is greatly improved. As shown in Fig. 8(c), there were some particles remained within the frame of dry foam, which further indicates that the particles are adhered to the bubble surface. If the particles are in the surrounding continuous phase rather than adsorbed on the bubble surface, they will be expelled with the liquid drainage rather than stayed inside the skeleton of dry foam.

3.4. Rheological characterization of bulk solution

In order to investigate the interaction between clay particles after the adsorption of AOS molecules, the rheological parameters of clay

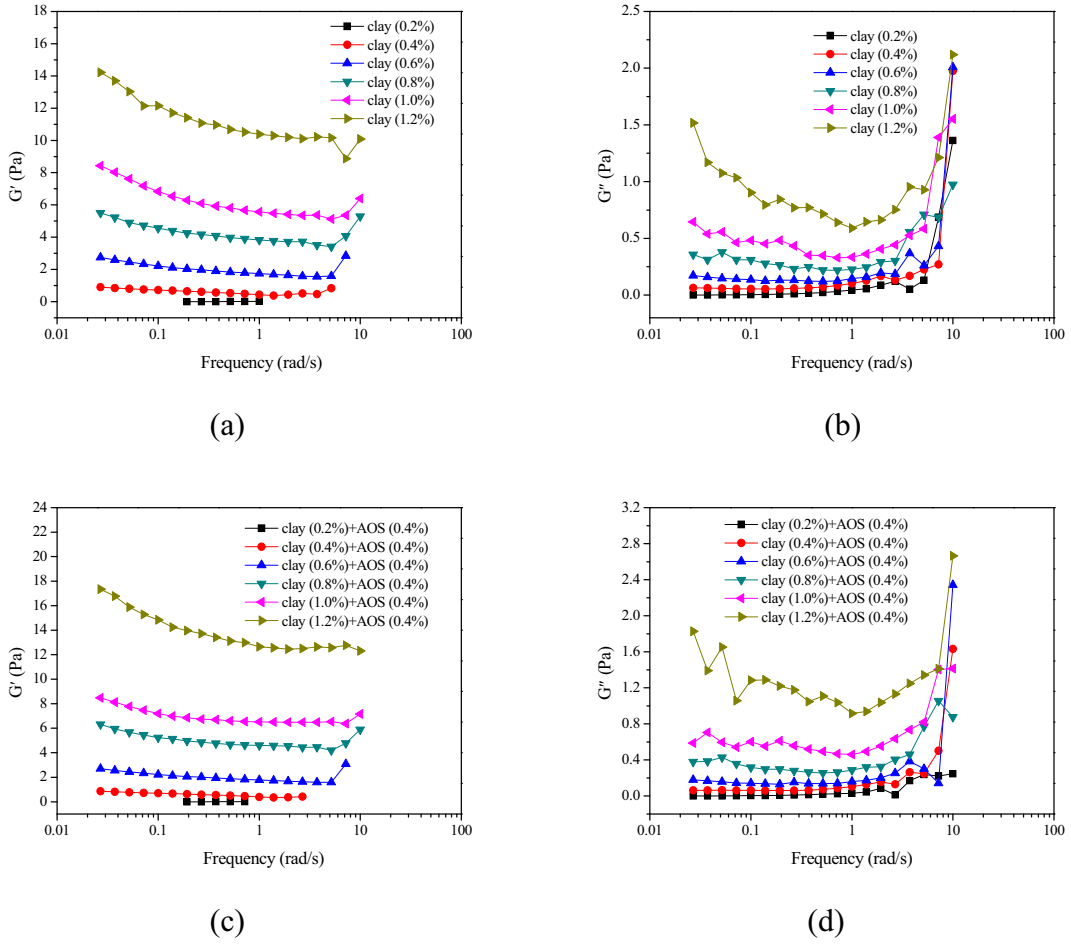

Fig. 10. G′ and G″ were a function of frequency for clay and AOS/clay dispersions. (a): G′ of clay dispersion; (b): G″ of clay dispersion; (c): G′ of AOS/clay dispersion; (d): G″ of AOS/clay dispersion.

and AOS/clay dispersions were measured. The viscoelasticity property of the systems can visually reflect the change of interparticle interaction force. The curves of apparent viscosity at different shear rates for clay and AOS/clay dispersions were depicted in Fig. 9. It could be seen that the apparent viscosity of clay dispersions decreased with the increase of shear rate, and the obtained viscosity curves are all typical shear thinning curves (Fig. 9(a)). All the samples exhibit a good fit to the typical behavior of pseudo-plastic fluid. This is because that the clay dispersions form a "card house" structure through the combination of the edges and surfaces of the granular lamella before sheared, which has a high strength of network structure and apparent viscosity. The micronetwork structure in the original systems will be destroyed gradually with the increase of shear rate, therefore, the viscosity of the systems decreases gradually. A similar viscosity curve was obtained for AOS/clay dispersions (Fig. 9(b)). Such shear thinning behavior is analogous to that of polymer solution in which the apparent viscosity exhibits a shear rate dependent manner. The orientation and movement of polymer molecules in bulk solution can be disturbed with increasing the shear rate. Such similar trend is also observed by the work of many others.

Furthermore, the apparent viscosity of bulk solution increased generally as the clay concentration increased, with the largest effects being observed at the higher clay concentration. The exact cause is unclear and no satisfactory explanation for this surprising behavior has been found up to now. This may be a combination of macromolecule chains that are reinforced at higher clay concentrations, resulting in a corresponding increase in apparent viscosity. The apparent viscosity for all samples was slightly increased when the shear rate higher than 50 s^{-1}. At low shear rate, high clay concentration represents the strong interaction between clay molecules, increasing the apparent viscosity of the bulk solution rapidly with the clay concentration. At high shear rate, the clay molecules are arranged along the flow direction and the resistance of all clay concentrations is similar. In addition, the introduction of AOS has little effect on the apparent viscosity of the solution.

Generally, the high plateau with complex modulus independent of the shear stress is considered to be a linear viscoelastic region. Therefore, before performing frequency oscillation measurements, the samples are always guaranteed to be in the linear viscoelastic region. The parameters G′ and G″ for all samples were measured in the range of 0.02–10.0 Hz using Haake MARS rheometer and the results were shown in Fig. 10. In contrast to G″, some data of G′ missed due to the detection limit of the instrument. At low clay concentrations, the values of the elastic and viscosity parts of viscoelastic moduli for all samples were small, and the values of G′ and G″ increased with the clay concentration. For clay dispersions, the results indicate that both G′ and G″ for all samples exhibit a good fit to "valley-shaped" response manner with the frequency, particularly the tendency of G″ with frequency is more obviously in high frequency. In addition, the values of G′ are always higher than that of G″ with the same clay concentration in the experimental frequency range. This phenomenon indicates that the elastic components predominate in viscoelasticity compared to viscosity component, and it can be inferred that a gel-like structure in the liquid may be formed. The gel-like structure can improve the foam stability by immobilizing solution droplets in the formed structure. Previous studies have also confirmed similar results [55,56]. Moreover, when the clay concentration exceeded 0.6 wt% in the AOS/clay dispersions, the values of G′ and G″ were higher than that of clay dispersions. The results reveal that there is synergistic effect between AOS and clay dispersion and the

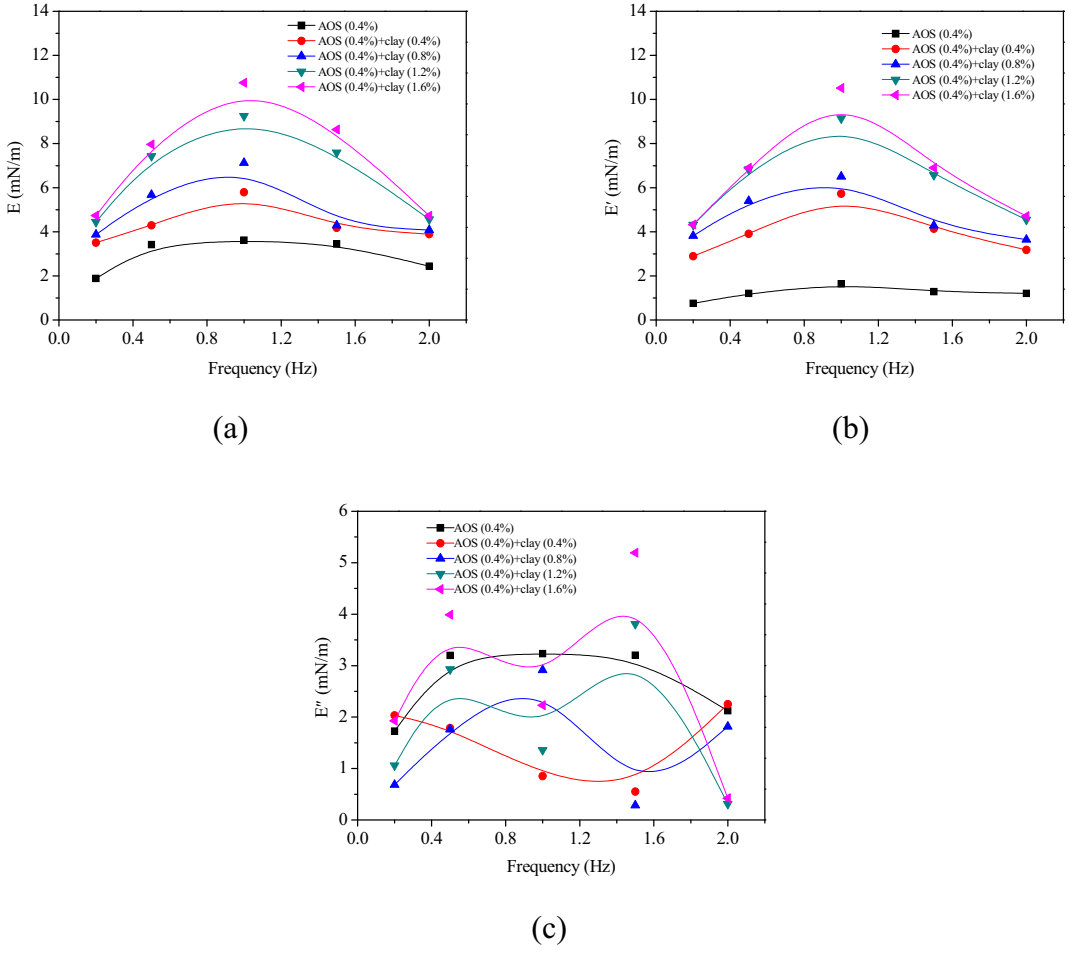

Fig. 11. (a) to (c) illustrates a plot of the overall modulus E, the storage modulus E′ and the loss modulus E″ as a function of frequency for AOS and AOS/clay liquid films.

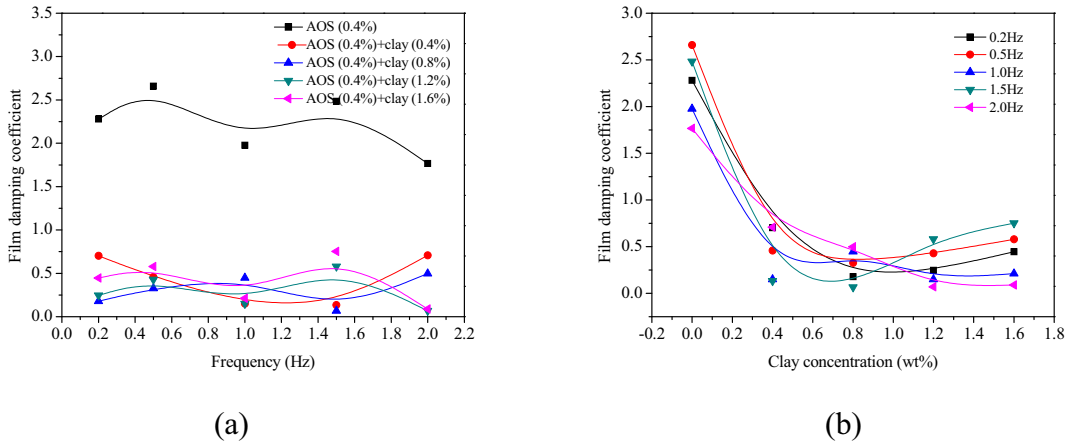

Fig. 12. The film damping coefficient as a function of frequency for AOS/clay (a) and as a function of clay concentration for AOS/clay.

viscoelasticity of AOS/clay dispersions is higher than that of clay dispersions. It is consistent with the stability of bulk foams that the AOS/clay foams are more stable than AOS foams. In addition, the dynamic modulus of AOS/clay dispersions is higher than that of clay dispersion, indicating that AOS/clay dispersions can bear larger stress.

3.5. The viscoelasticity modulus of liquid films

Previous studies indicate that the viscoelasticity of liquid films plays a significant role in foam stability. When foam passes through the porous media throat, the liquid films will expand or extract. The homemade FL10A extensional viscoelasticity meter was used to simulate the expanding and extracting process of liquid films.

The results of the E, E′ and E″ for AOS/clay liquid films were shown in Fig. 11. For AOS/clay liquid films, along with the increase of frequency, the values of E and E′ increased gradually and reached a maximal value at the frequency of 1.0 Hz then decreased again. For E″, it cannot find the direct relationship between the loss modulus and frequency. For AOS liquid film, the values of E′ were always lower than that of E″, which indicates that the viscous is predominant in AOS liquid film in contrast to the elastic. While for the AOS/clay liquid films, the values of E′ were larger than that of E″ in general except some data. The results demonstrate that the liquid films are more elastic rather than viscous after adding the clay particles in the dispersions. Furthermore, the value of film damping coefficient tanθ for AOS liquid film was >1.0 (Fig. 12(a)), while the AOS/clay liquid films tanθ was <1.0. Thus, compared with the AOS/clay liquid films, the energy loss portion is higher for AOS liquid film when the same total energy from outward is introduced into films. This phenomenon demonstrates that more energy from the outside will be availably used for AOS liquid film after the addition of clay particles.

Moreover, both the values of E and E′ for AOS/clay liquid films improved obviously after the introduction of clay particles into the dispersions, as compared to the pure AOS liquid film. As a result, the stability of liquid films is improved. The values of E increased with the clay concentration and the same trend is found between E′ and clay concentration. While for E″, the effect of clay concentration on the viscous component of liquid films is unclear and no correlation is found. The value of film damping coefficient tanθ decreased with the increase of clay concentration (Fig. 12(b)), which shows that more energy portion from outward is accumulated for AOS/clay liquid films. As the clay concentration reached 0.8 wt%, equilibrium value (from 0.5 to 0.7) of film damping coefficient tanθ was found in the range of 0.2 Hz to 2.0 Hz. Thus, when the clay particles reach the equilibrium level, more clay particles introduced into the liquid films is not favored and high concentration clay contributes a little to energy distribution. It indicates that the additional energy from outward introduced into the liquid films will not be effectively utilized when the equilibrium value of film damping coefficient tanθ is obtained, even if the values of viscoelasticity modulus are higher in the high concentration clay dispersions.

4. Conclusions

In the present study, the stability and rheological behavior of foams prepared by AOS surfactant and clay particle dispersions are investigated in detail. More stable foams can be formed from the AOS/clay dispersions due to the synergistic effect of AOS surfactant with the clay particles, and the most stable foam is obtained at 1.0 wt% of AOS in AOS/clay dispersions. Compared with surface charge, the hydrophobicity of particles directly influences the foam stability and the most hydrophobic clay particles in AOS/clay dispersions own the most stable foams. Laser-induced confocal scanning microscopy experiments reveal that the AOS-modified particles are adsorbed on the bubble surface and the three-dimensional network structure is formed between the armored bubbles, thus the foam stability increases. In addition, the rheological behavior studies demonstrate that the viscoelasticity modulus of both liquid film and bulk solution for AOS surfactants are enhanced after the addition of clay particles, in which the viscoelasticity behavior dominated by elastic modulus, thereby increasing the foam stability. The film damping coefficient indicates that more energy from outside will be availably used for AOS liquid film after the addition of clay particles.

Acknowledgements

The authors would like to thank others in State Key Laboratory of Enhanced Oil Recovery in Research Institute of PetroChina Exploration and Development helping with the experiment research. And the authors would like to acknowledge the China National Science and Technology major project 2011ZX05010-005 for its support of this project.

References

[1] S. Thomas, Enhanced oil recovery-an overview, Oil Gas Sci. Technol. 63 (2007) 9–19.
[2] J.J. Taber, Research on enhanced oil recovery: past, present and future, Pure Appl. Chem. 52 (1980) 1323–1347.
[3] M.S. Kamal, A review of gemini surfactants: potential application in enhanced oil recovery, J. Surfactant Deterg. 19 (2016) 223–236.
[4] A.A. Olajire, Review of ASP EOR (alkaline surfactant polymer enhanced oil recovery) technology in the petroleum industry: prospects and challenges, Energy 77 (2014) 963–982.
[5] R. Farajzadeh, A. Andrianov, R. Krastev, G.J. Hirasaki, W.R. Rossen, Foam-oil interaction in porous media: implications for foam assisted enhanced oil recovery, Adv. Colloid Interfac. 183–184 (2012) 1–13.
[6] A. Andrianov, R. Farajzadeh, M.M. Nick, M. Talanana, P.L.J. Zitha, Immiscible foam for enhancing oil recovery: bulk and porous media experiments, Ind. Eng. Chem. Res. 51 (2012) 2214–2226.

[7] P. Wei, W. Pu, L. Sun, Y. Pu, S. Wang, Z.K. Fang, Oil recovery enhancement in low permeable and severe heterogeneous oil reservoirs via gas and foam flooding, J. Pet. Sci. Eng. 163 (2018) 340–348.
[8] C. Huh, W.R. Rossen, Approximate pore-level modeling for apparent viscosity of polymer-enhanced foam in porous media, SPE J. 13 (2008) 17–25.
[9] T. Zhu, D.O. Ogbe, S. Khataniar, Improving the foam performance for mobility control and improved sweep efficiency in gas flooding, Ind. Eng. Chem. Res. 43 (2004) 4413–4421.
[10] G.Q. Jian, M.C. Puerto, A. Wehowsky, P.F. Dong, K.P. Johnston, G.J. Hirasaki, Static adsorption of an ethoxylated nonionic surfactant on carbonate minerals, Langmuir 32 (2016) 10244–10252.
[11] F. Guo, S.A. Aryana, Improved sweep efficiency due to foam flooding in a heterogeneous microfluidic device, J. Pet. Sci. Eng. 164 (2018) 155–163.
[12] T.C. Ransohoff, C.J. Radke, Mechanisms of foam generation in glass-bead packs, Soc. Pet. Eng. 3 (1988) 73–585.
[13] R. Rafati, O.K. Oludara, A.S. Haddad, H. Hamidi, Experimental investigation of emulsified oil dispersion on bulk foam stability, Colloids Surf. A Physicochem. Eng. Asp. 554 (2018) 110–121.
[14] D.L. Manyala, G. Rajput, N. Pandya, D. Varade, Enhanced foamability and foam stability of polyoxyethylene cholesteryl ether in occurrence of ionic surfactants, Colloids Surf. A Physicochem. Eng. Asp. 551 (2018) 81–86.
[15] O.A. Saavedra, J.G. Fadrique, Surface tension and foam stability prediction of polydimethylsiloxane-polyol systems, Open J. Phys. Chem. 2 (4) (2012) 189–194.
[16] J.S. Chen, Z.A. Jiang, L. Jiang, Experiments on the foaming agent formula of froth dedusting during down-the-hole drilling in open-pit mine, J. China Coal Soc. 40 (2015) 407–412.
[17] Y. Liu, Q. Li, A.G. Yao, X.Y. Zhang, Experiments for selecting the optimal foam drilling fluid formula, Chem. Tech. Fuels Oil. 52 (3) (2016) 340–345.
[18] S.Y. Chen, G.Q. Jian, Q.F. Hou, S.L. Gao, Y.S. Luo, Y.Y. Zhu, W.J. Li, Effect of oil on the stability of polymer enhanced foams, Int. J. Oil Gas Coal T. 6 (2013) 675–688.
[19] A. Bureiko, A. Trybala, N. Kovalchuk, V. Starov, Current applications of foams formed from mixed surfactant-polymer solutions, Adv. Colloid Interf. Sci. 222 (2015) 670–677.
[20] G.Q. Jian, Q.F. Hou, Y.Y. Zhu, Stability of polymer and surfactant mixture enhanced foams in the presence of oil under static and dynamic conditions, J. Disper. Sci. Technol. 36 (2015) 477–488.
[21] P. Wei, W. Pu, L. Sun, Y. Pu, D.B. Li, Y. Chen, Role of water-soluble polymer on foam-injection process for enhancing oil recovery, J. Ind. Eng. Chem. 65 (2018) 280–289.
[22] T.N. Hunter, R.J. Pugh, G.V. Franks, G.J. Jameson, The role of particles in stabilising foams and emulsions, Adv. Colloid Interf. Sci. 137 (2) (2008) 57–81.
[23] M. Siva, K. Ramamurthy, R. Dhamodharan, Sodium salt admixtures for enhancing the foaming characteristics of sodium lauryl sulphate, Cement Concrete Comp. 57 (2015) 133–141.
[24] G. Bournival, Z. Du, S. Ata, G.J. Jameson, Foaming and gas dispersion properties of non-ionic surfactants in the presence of an inorganic electrolyte, Chem. Eng. Sci. 116 (2014) 536–546.
[25] S. Kumar, A. Mandal, Studies on interfacial behavior and wettability change phenomena by ionic and nonionic surfactants in presence of alkalis and salt for enhanced oil recovery, Appl. Surf. Sci. 372 (2016) 42–51.
[26] O. Paulson, R.J. Pugh, Flotation of inherently hydrophobic particles in aqueous solutions of inorganic electrolytes, Langmuir 12 (1996) 4808–4813.
[27] S. Ata, P.D. Yates, Stability and flotation behaviour of silica in the presence of a nonpolar oil and cationic surfactant, Colloids and Surfaces A: Physicochem. Eng. Aspects 277 (2006) 1–7.
[28] M. Veyskarami, M.H. Ghazanfari, Synergistic effect of like and opposite charged nanoparticle and surfactant on foam stability and mobility in the absence and presence of hydrocarbon: a comparative study, J. Pet. Sci. Eng. 166 (2018) 433–444.
[29] Z.L. Xi, L.W. Jin, L.J.Y. Richard, D. Li, Characteristics of foam sol clay for controlling coal dust, Powder Technol. 335 (2018) 401–408.
[30] S.U. Pickering, Pickering: emulsions, J. Chem. Soc. Trans. 91 (1907) 2001–2021.
[31] B.P. Binks, S.O. Lumsdon, Picketing emulsions stabilized by monodisperse latex particles: effects of particle size, Langmuir 17 (15) (2001) 4540–4547.
[32] I. Kim, A.J. Worthen, K.P. Johnston, D.A. DiCarlo, C. Huh, Size-dependent properties of silica nanoparticles for Pickering stabilization of emulsions and foams, J. Nanopart. Res. 18 (2016) 1–12.
[33] N. Yekeen, M.A. Manan, A.K. Idris, E. Padmanabhan, R. Junin, A.M. Samin, A.O. Gbadamosi, I. Oguamah, A comprehensive review of experimental studies of nanoparticles-stabilized foam for enhanced oil recovery, J. Petrol. Sci. Eng. 164 (2018) 43–74.
[34] S. Babamahmoudi, S. Riahi, Application of nano particle for enhancement of foam stability in the presence of crude oil: experimental investigation, J. Mol. Liq. 264 (2018) 499–509.
[35] B.P. Binks, Particles as surfactants-similarities and differences, Curr. Opin. Colloid In. 7 (2002) 21–41.
[36] L. Jiang, S. Li, W. Yu, J. Wang, Q. Sun, Z. Li, Interfacial study on the interaction between hydrophobic nanoparticles and ionic surfactants, Colloids and Surfaces A: Physicochem. Eng. Aspects 488 (2016) 20–27.
[37] M.A. Ahmadi, S.R. Shadizadeh, Adsorption of novel nonionic surfactant and particles mixture in carbonates: enhanced oil recovery implication, Energy Fuel 26 (8) (2012) 4655–4663.
[38] U.T. Gonzenbach, A.R. Studart, E. Tervoort, L.J. Gauckler, Ultrastable particle-stabilized foams, Angew. Chem. Int. Edit. 45 (2006) 3526–3530.
[39] A. Stocco, J. Crassous, A. Salonen, A.S. Jalmes, D. Langevin, Two-mode dynamics in dispersed systems: the case of particle-stabilized foams studied by diffusing wave spectroscopy, Phys. Chem. Chem. Phys. 13 (8) (2011) 3064–3072.
[40] X. Zhong, D.X. Liu, X.F. Shi, H.T. Zhao, C. Pei, T.Y. Zhu, M.L. Shao, F. Zhang, Characteristics and functional mechanisms of clay-cement stabilized three-phase nitrogen foam for heavy oil reservoir, J. Pet. Sci. Eng. 170 (2018) 497–506.
[41] S. Abend, N. Bonnke, U. Gutschner, G. Lagaly, Stabilization of emulsions by heterocoagulation of clay minerals and layered double hydroxides, Colloid Polym. Sci. 276 (1998) 730–737.
[42] D.E. Tambe, M.M. Sharma, The effect of colloidal particles on fluid-fluid interfacial properties and emulsion stability, Adv. Colloid Interfac. 52 (1994) 1–63.
[43] G.Q. Jian, Q.F. Hou, S.Y. Chen, D.H. Wang, Y.S. Luo, Z. Wang, Y.Y. Zhu, Comparative study of extensional viscoelasticity properties of liquid films and stability of bulk foams, J. Disper. Sci. Technol. 34 (2013) 1382–1391.
[44] S.Y. Chen, Q.F. Hou, Y.Y. Zhu, D.H. Wang, W.J. Li, On the origin of foam stability: understanding from viscoelasticity of foaming solutions and liquid films, J. Disper. Sci. Technol. 35 (2014) 1214–1221.
[45] S.Y. Chen, Y.J. Zhou, G.H. Wang, W.J. Li, Y.Y. Zhu, J.A. Zhang, Influence of foam apparent viscosity and viscoelasticity of liquid films on foam stability, J. Disper. Sci. Technol. 37 (2016) 479–485.
[46] S.Y. Zhang, Q. Lan, Q. Liu, J. Xu, D.J. Sun, Aqueous foams stabilized by Laponite and CTAB, Colloids Surf. A: Physicochem. Eng. Aspects 317 (2008) 406–413.
[47] T. Sharma, G.S. Kumar, B.H. Chon, J.S. Sangwai, Viscosity of the oil-in-water Pickering emulsion stabilized by surfactant-polymer and nanoparticle-surfactant-polymer system, Korea-Aust. Rheol. J. 26 (4) (2014) 377–387.
[48] D.H. Wang, Q.F. Hou, Y.S. Luo, Y.Y. Zhu, H.F. Fan, Blocking ability and flow characteristics of nitrogen foam stabilized with clay particles in porous media, J. Disper. Sci. Technol. 36 (2015) 170–176.
[49] E. Tombácz, M. Szekeres, Surface charge heterogeneity of kaolinite in aqueous suspension in comparison with montmorillonite, Appl. Clay Sci. 34 (2006) 105–124.
[50] G.Q. Jian, M.C. Puerto, A. Wehowsky, P.F. Dong, K.P. Johnston, G.J. Hirasaki, S.L. Biswal, Static adsorption of an ethoxylated nonionic surfactant on carbonate minerals, Langmuir 32 (40) (2016) 10244–10252.
[51] G.Q. Jian, M. Puerto, A. Wehowsky, C. Miller, G.J. Hirasaki, S.L. Biswal, Characterizing adsorption of associating surfactants on carbonates surfaces, J. Colloid Interf. Sci. 513 (2018) 684–692.
[52] E.H. Hill, Y. Zhang, D.G. Whitten, Aggregation of cationic p-phenylene ethynylenes on Laponite clay in aqueous dispersions and solid films, J. Colloid Interf. Sci. 449 (2015) 347–356.
[53] G. Kaptay, Interfacial criteria for stabilization of liquid foams by solid particles, Colloids Surf. A: Physicochem. Eng. Aspects 230 (2004) 67–80.
[54] B.P. Binks, P.D.I. Fletcher, Particles adsorbed at the oil-water interface: a theoretical comparison between spheres of uniform wettability and 'Janus' particles, Langmuir 17 (16) (2001) 4708–4710.
[55] Y. Nitta, R. Takahashi, K. Nishinari, Viscoelasticity and phase separation of aqueous Na-type gellan solution, Biomacromolecules 11 (2009) 187–191.
[56] M.C. Alfaro, A.F. Guerrero, J. Munoz, Dynamic viscoelasticity and flow behavior of a polyoxyethylene glycol nonylphenyl ether/toluene/water system, Langmuir 16 (2000) 4711–4719.